Research Results in Pharmacology

Research Results in Pharmacology 10(4): 87–97
UDC: 615.015; 543.51+543.54
DOI 10.18413/rrpharmacology.10.547

Research Article

The influence of exogenous recombinant HSP 70 on the alteration of membrane stiffness in hippocampal neurons following the modeling of neonatal hypoxic-ischemic injury in mice

Vladimir M. Pokrovsky[1], Alexey V. Deikin[1], T. Zhang[2], Nikolai A. Verlov[3,4], Andrey L. Konevega[3], Mikhail V. Korokin[1]

1 Belgorod State National Research University, 85 Pobedy St., Belgorod 308015 Russia
2 College of Life Sciences, Dezhou University, Dezhou 253023 China
3 Petersburg Nuclear Physics Institute named by B.P. Konstantinov of National Research Centre «Kurchatov Institute», 1 Orlova Grove, Leningrad region, Gatchina 188300 Russia
4 National Research Centre «Kurchatov Institute», 1 Russia Akademika Kurchatov Square, Moscow 123098 Russia

Corresponding author: Vladimir M. Pokrovsky (vmpokrovsky@yandex.ru)

Academic editor: Oleg Gudyrev ♦ **Received** 11. October 2024 ♦ **Accepted** 31 October 2024 ♦ **Published** 30 December 2024

Citation: Pokrovsky VM, Deikin AV, Zhang T, Verlov NA, Konevega AL, Korokin MV (2024) The influence of exogenous recombinant HSP 70 on the alteration of membrane stiffness in hippocampal neurons following the modeling of neonatal hypoxic-ischemic injury in mice. Research Results in Pharmacology 10(4): 87–97. https://doi.org/10.18413/rrpharmacology.10.547

Abstract

Introduction: The use of atomic force microscopy (AFM) to investigate membrane stiffness in neurons provides valuable insights into cellular mechanisms and their alterations in response to various pathophysiological conditions. Heat shock protein HSP 70, a component of the cellular stress response system, plays a role in stabilizing the protein structures of cellular organelles. However, studies examining changes in the stiffness of hippocampal neuronal membranes in its presence, particularly following cerebral circulation disturbances, have not been conducted yet.

Materials and Methods: The study was performed on a mixed culture of hippocampal neurons derived from 9-day-old male CD-1 mice, obtained 24 hours after modeling neonatal hypoxia-ischemia. The following groups were formed: Intact culture; HI culture; HI + rhHSP70 10^{-6} M; HI + rhHSP70 10^{-8} M; HI + rhHSP70 10^{-9} M; HI + rhHSP70 10^{-12} M, with the substance added in dilutions from an initial dose of 0.1 µg/g. The Young's modulus was measured using force spectroscopy, and maps of local stiffness of various surface areas were generated.

Results and Discussion: The neonatal hypoxia-ischemia model resulted in an 18% increase in the stiffness of the neuronal cell surface compared to the control group ($p<0.001$). The addition of rhHSP70 at concentrations of 10^{-6} M and 10^{-8} M to the HI culture led to an increase in membrane stiffness by 20% ($p<0.001$) and 3% ($p<0.0034$), respectively, while dilutions of rhHSP70 at 10^{-9} M and 10^{-12} M resulted in a decrease in membrane stiffness by 35% ($p<0.001$) and 22% ($p<0.001$) compared to the intact group, respectively. In comparison to such in the neuronal culture group after neonatal hypoxia-ischemia modeling, membrane stiffness with the addition of rhHSP70 at 10^{-8} M, 10^{-9} M, and 10^-12 M decreased by 17% ($p<0.0004$), 65% ($p<0.001$), and 49% ($p<0.001$), respectively.

Conclusion: Thus, the addition of rhHSP 70 results in a reduction in membrane stiffness in the mixed culture of hippocampal neurons in mice, compared to the intact culture obtained after neonatal hypoxia-ischemia. The AFM method allows for the assessment of how various molecules, such as heat shock proteins (e.g., rhHSP70), influence the mechanical properties of membranes, which may be critically important for the development of new therapeutic agents.

Graphical abstract

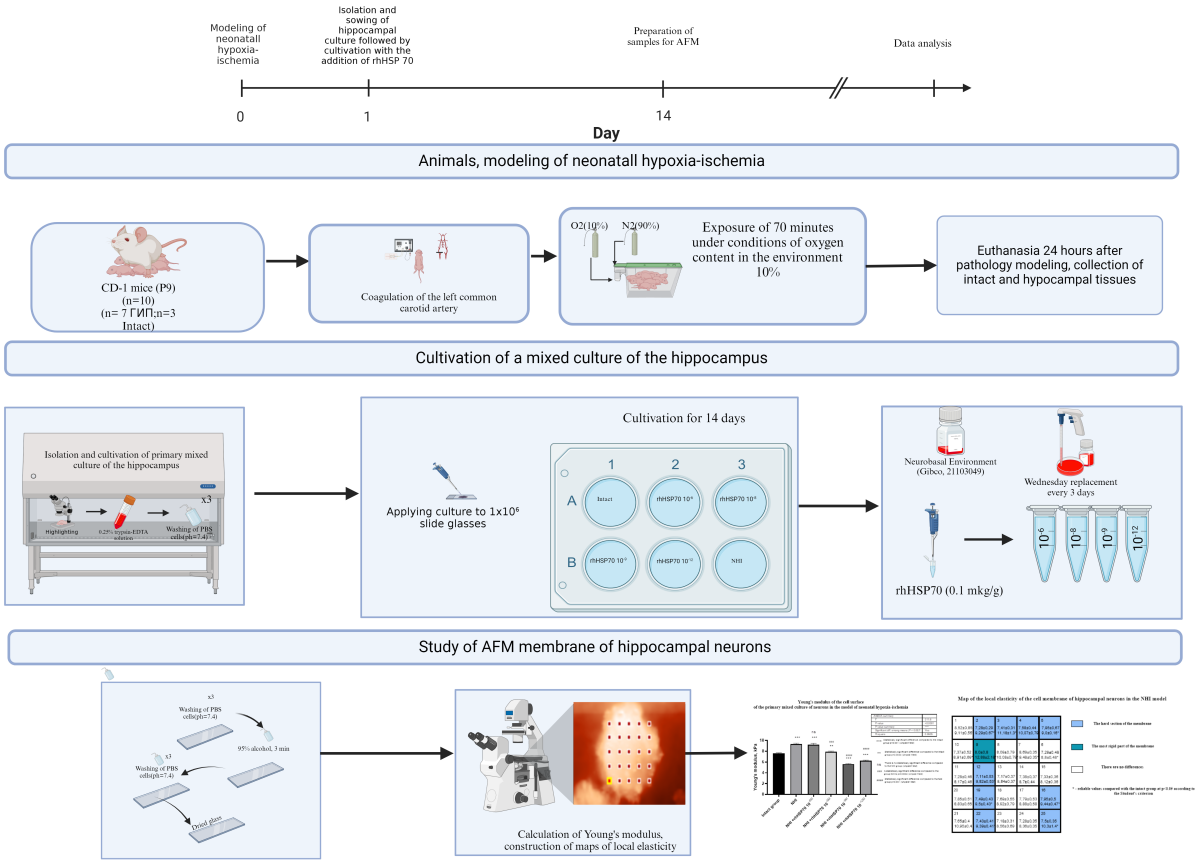

Keywords

HSP 70, fetal hypoxia-ischemia, Young's modulus, hippocamp neuron membrane, AFM

Introduction

The application of atomic force microscopy (AFM) to study membrane stiffness in neurons opens new horizons for understanding the complex mechanisms underlying neuronal function and their alterations in disease states (Frederix et al. 2009). Contemporary research has placed significant emphasis on the biochemical aspects of neuronal death in hypoxic and ischemic conditions, while less attention has been paid to biophysical factors (Bryniarska-Kubiak et al. 2023), including cytoskeletal organization and the mechanical properties of cells (Tuo et al. 2021). The forces generated by the cellular cytoskeleton and/or extracellular matrix (Chaudhuri 2018; Guimarães et al. 2020) are crucial not only in the process of embryonic development, where they influence cell proliferation and differentiation (Vining and Mooney 2017), but are also characteristic of pathological processes, including those related to the brain (Handorf et al. 2015). The organization and proper functioning of the cytoskeleton are essential for effective signal transduction from the cellular environment to the nucleus (Oashi et al. 2017). It is known that mechanical signal transduction occurs 40 times faster than the transduction of biochemical signals within the cytoplasm. Thus, any alteration in the integrity and functioning of the cytoskeleton can lead to various disruptions, resulting in impaired homeostatic regulation. Conversely, the interaction of the cytoskeleton with physical factors plays a key role in regulating the formation of new neurons (Chighizola et al. 2019; Seano et al. 2019) discovered that forces generated by solid stress lead to changes in nuclear morphology and subsequent neuronal death in regions subjected to deformation caused by brain tumor mass. Furthermore, the solid stress generated by the tumor may reduce perfusion in surrounding blood vessels. Changes in brain stiffness have been observed in C57BL/6 mice subjected to middle cerebral artery occlusion (MCAo), likely due to alterations in fluid distribution caused by brain damage (Sun et al. 2023). Considering the physical mechanisms of brain injury resulting from the interaction of forces arising under pathological conditions, the search for similar foundations in the case of ischemic stroke may represent an intriguing avenue for research.

Heat shock protein HSP 70, a component of the cellular stress response system, plays a role in stabilizing the protein structures of cellular organelles. However, studies examining changes in the stiffness of hippocampal neuronal membranes in its presence as a therapeutic agent in conditions associated with cerebral circulation disturbances have not been conducted.

Objective of the Study: The objective of this study is to evaluate the changes in membrane stiffness of mixed cultures of hippocampal neurons in the presence of rhHSP70 using atomic force microscopy methods after modeling neonatal hypoxia-ischemia in mice.

Materials and Methods

Animals

The animals were housed under SPF conditions in the vivarium of Belgorod State National Research University (Belgorod State University) with artificially regulated light cycles (12 hours of darkness and 12 hours of light) at a temperature ranging from +22 to +26°C, with free access to food and water. The study adhered to ethical principles for the care and use of laboratory animals in accordance with the European Convention for the Protection of Vertebrate Animals Used for Experimental and Other Scientific Purposes (ETS No. 170). All painful procedures involving the animals were conducted in compliance with regulatory standards: Directive 2010/63/EU of the European Parliament and Council of the European Union dated September 22, 2010, On the Protection of Animals Used for Scientific Purposes. The study was approved by the Animal Care and Use Committee of Belgorod State National Research University, expert opinion No. 01-06i/24 dated June 3, 2024.

Study design

Groups and neonatal hypoxia-ischemia model

The experiment utilized 9-day-old male CD-1 mice (n=10). The modeling of neonatal hypoxia-ischemia (HI) was performed using the Rice-Vannucci modification as previously described (n=7) (Sheldon et al. 2019). Briefly, the left common carotid artery was coagulated under inhalational anesthesia with isoflurane (4% for induction and 1.2% for maintenance). Following the procedure, the animals were returned to nursing staff for two hours and then placed in the conditions of reduced oxygen concentration in the environment by displacing it with nitrogen (10% O2; 90% N2). The gas composition within the chamber was monitored using a gas analyzer PKG-4 B-K-P (62615-15 until November 12, 2025; EXCIS; RF). The control group consisted of three intact animals (Fig.1, p.1).

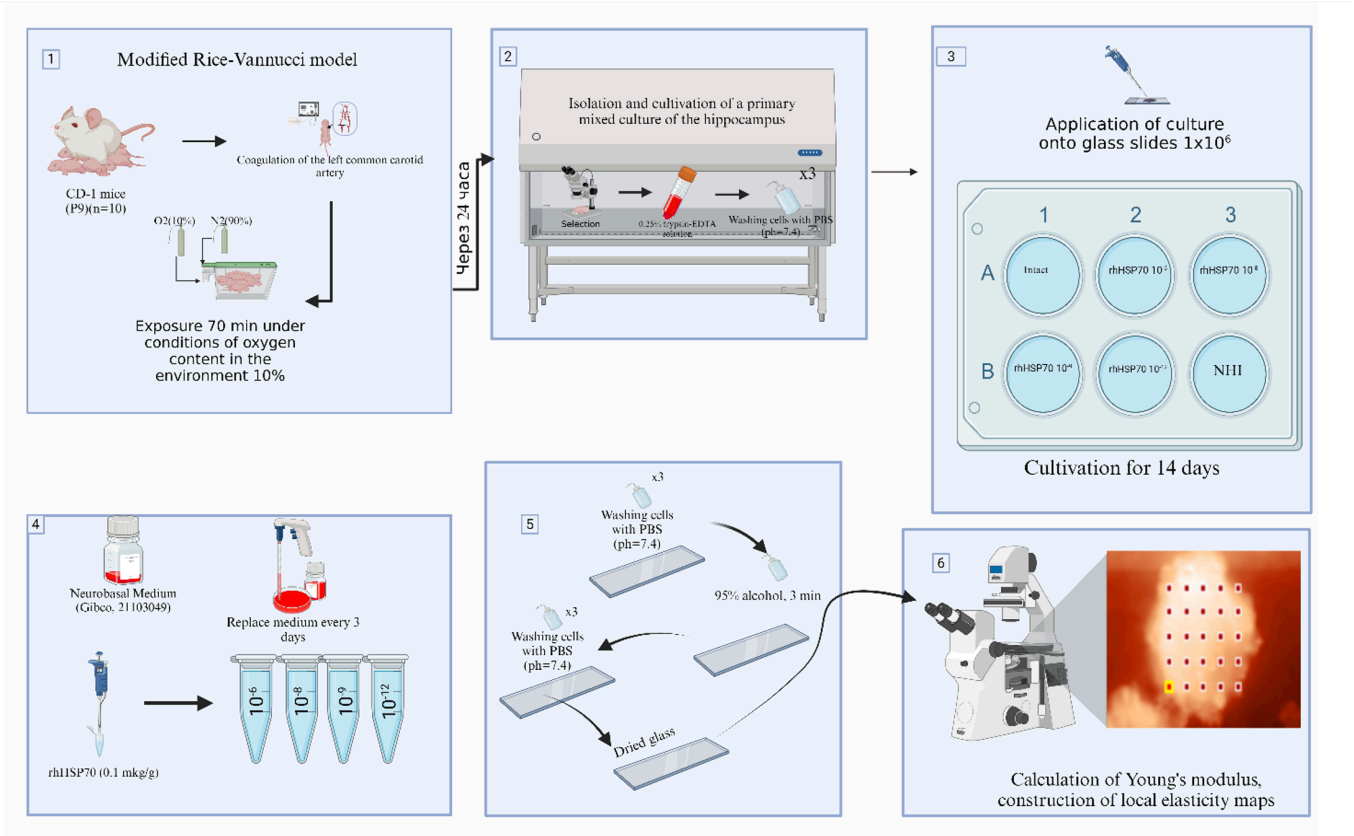

Figure 1. Study Design. Note: 1 - Modeling of fetal hypoxia-ischemia; 2 - Isolation of primary HIppocampal cultures; 3,4 - Cultivation of cultures; 5 - Sample preparation for atomic force microscopy (AFM); 6 - Measurement of Young's modulus using AFM in force spectroscopy mode. Description provided in the text.

Isolation and cultivation of primary mixed cultures of hippocampal neurons

Euthanasia of the animals was performed by decapitation, after which the brain was extracted and placed in a Petri dish with cooled phosphate-buffered saline (PBS) at pH=7.4. Under a binocular microscope (Leica, magnification ×4), the large cerebral hemispheres were separated. The hippocampus was placed on a microscope slide with a "well" and minced into 6-8 pieces, which were then transferred to a tube containing 0.25% trypsin-EDTA solution (Gibco, 25200056). The tissue was trypsinized in 0.25% trypsin-EDTA solution for 20 minutes at 37ºC in a 5% CO2 incubator (Binder, Germany). After trypsinization, the cell suspension was washed three times with PBS. To the resulting suspension, 2 mL of neurobasal medium (Gibco, 21103049) containing 2% B-27 supplement (Gibco, 17504044), 0.5 mM of L-Glutamax (Gibco, 25030081), 10% fetal bovine serum (PanEco), and 1% PenStrep (PanEco) was added (Fig. 1.2).

The primary mixed culture of hippocampal neurons was cultivated on glass slides that had been previously degreased in concentrated hydrochloric acid for 24 hours and baked at 200°C for 2 hours. The cell seeding density was 1×10^6 cells per slide. The slides were placed in 6-well plates, to which neurobasal medium for cultivation was added, supplemented with rhHSP70 protein from E. coli BL21 at a dose of 0.1 µg/ml, obtained from a research team led by M.B. Evgen'ev (V.A. Engelhardt Institute of Molecular Biology, Russian Academy of Sciences) (Demyanenko S. et al., 2021). The neurobasal medium for cultivation contained 2% B-27 supplement, 0.5 mM L-Glutamax (Gibco, 25030081), 5% fetal bovine serum (PanEco), and 1% PenStrep (PanEco). The cultivation was carried out for 14 days, with half of the medium replaced with freshly prepared medium every 3 days. At the end of the differentiation period on day 14, samples for atomic force microscopy (AFM) were prepared (Fig. 1.3-4).

Thus, the following groups of the studied culture were formed:

Intact culture
HI culture
HI culture + rhHSP70 10^{-6} M
HI culture + rhHSP70 10^{-8} M
HI culture + rhHSP70 10^{-9} M
HI culture + rhHSP70 10^{-12} M
Sample Preparation for AFM

The culture medium was removed from the wells of the plate, and the slides were washed three times with PBS (pH = 7.4). Then, 95% ethanol was applied to the slides until the surface was fully covered, and the preparation was fixed for 3 minutes. After the fixation time, the preparations were washed three times with PBS and then rinsed with distilled water. The slides were dried in a laminar flow hood and subsequently scanned using an atomic force microscope (Fig. 1, p. 5).

Measurement of Young's modulus using AFM in force spectroscopy mode

The method for measuring Young's modulus, which quantitatively characterizes cell stiffness, is based on measuring the degree of deformation of the sample surface during its interaction with the AFM probe tip (Cartagena-Rivera et al. 2015) (Fig. 1,6). Scanning was performed in force spectroscopy mode with a scan frequency of 0.6–0.8 Hz, using an NSG03 cantilever (Nanoworld, USA) with a stiffness of 1.1 N/m and a tip radius of 10 nm. The mechanical properties of the surface were assessed in localized areas according to the local elasticity maps. For this, a load was applied to 25 localized areas of the cell surface.

The Young's modulus was calculated according to an algorithm previously published (Skorkina et al. 2012). To calculate Young's modulus, the force curves obtained in the experiment were transformed from the D-z coordinate system to the F-Δh system, where D is the current disbalance photodiode, z is the distance between the cantilever moves via the AFM piezo scanner when approaching the surface. The transformation procedure was performed using the DFL_to_Force script of the Nova software (NT-MDT, Zelenograd, 2009). On the transformed force curves, values of DX (nm), DY (nN), and Y (nN) were found, from which the penetration depth of the probe into the sample was calculated (formula 1):

$$x = \frac{\Delta Z(SetPoint - DFL0)}{\Delta DFL} \quad (1),$$

where ΔZ is the transformed value of the force curve by DX (nm); SetPoint is a functional parameter that defines the magnitude of the input signal of the feedback circuit during scanning (nA); DFL0 is the transformed value of the force curve by Y (nA); ΔDFL is the transformed calibration value of the force curve by DY (nN).

The force applied by the probe to the sample was calculated according to Hooke's law (formula 2):

$$F = k \times x \quad (2),$$

where k is the stiffness of the probe; x is the penetration depth of the probe into the sample.

Young's modulus was calculated using the following formula 3:

$$x = \frac{(4\sqrt{R})}{3E\Delta h(3/2)} \quad (3),$$

where F is the force with which the probe acts on the sample, nN; R is the radius of curvature of the probe, nm; E is Young's modulus, kPa; Δh is the depth of probe penetration into the sample, nm.

Statistical analysis of data

The analysis of each sample included the measurement of parameters from 20 cells. The total number of measurements conducted was 1000. The obtained data were checked for normal distribution. The significance of differences between groups treated with rhHSP70 and the intact and HI groups was calculated using an unpaired Student's t-test at $p < 0.05$. ANOVA was used to compare data between groups. Graphical illustrations and statistical processing were performed using GraphPad Prism 8 (GraphPad Software, CA, USA).

Results and Discussion

Young's modulus

The data characterizing the overall value of Young's modulus from the cell surface of neurons are presented in

Figure 2.

The overall value of Young's modulus from the cell surface of neurons in the intact group was 7.62 ± 0.09 kPa. The hypoxia-ischemia model in fetuses caused an 18% increase in cell surface stiffness ($p < 0.001$) compared to such in the control group ($p < 0.001$). When adding rhHSP70 at a concentration of 10^{-6} M to the HI culture, no significant differences were noted compared to the HI group, but compared to the intact group, membrane stiffness significantly increased by 20% ($p < 0.001$). Cultivating HI hippocampal neurons with rhHSP70 at a concentration of 10^{-8} M resulted in a 3% increase in membrane stiffness compared to the intact group ($p < 0.0034$), while compared to the HI group, the value decreased by 17% ($p < 0.0004$). Adding rhHSP70 at a concentration of 10^{-9} M to the HI culture resulted in a 35% decrease in membrane stiffness compared to such in the intact group ($p < 0.001$) and a 65% decrease ($p < 0.001$) compared to such in the HI group. Cultivating HI hippocampal neurons with rhHSP70 at a concentration of 10^{-12} M led to a 22% reduction in membrane stiffness ($p < 0.001$) compared to rhat in the intact group and a 49% reduction ($p < 0.001$) compared to that in the HI group.

Under hypoxic stress, there is an increase in the stiffness of the cell surface of hippocampal neurons. The addition of the exogenous heat shock protein HSP70 to the culture medium reduces cell surface stiffness, with the most pronounced effect observed at a concentration of 10^{-9} M.

Local elasticity maps

Local elasticity maps were created to represent data on the localized changes in membrane stiffness across the groups (Fig. 2–6).

The constructed maps of local elasticity demonstrate that under hypoxic conditions, the stiffness of the cell surface increased at all points of nanoindentation compared to that in the control (Fig. 3). The most rigid areas of the surface are observed at the periphery of the cell (points 3, 21, 25) and in the perinuclear space (point 9).

Under the influence of HSP70 at a concentration of 10^{-6} M, an increase in the stiffness of the neuronal cell surface was noted at the cell periphery in points 2, 3, 4, 6, and 15, with increases of 48.7%, 29%, 17%, 32%, and 50.6% ($p < 0.05$) respectively compared to the control. In the submembranous region at the periphery, point 15 exhibited a 36% increase in surface stiffness ($p < 0.05$) compared to that in cells subjected to hypoxia (Fig. 4).

Under the influence of HSP70 at a concentration of 10^{-6} M, an increase in stiffness was observed in the nuclear region at points 9, 13, 14, and 17, with respective increases of 63.6%, 26%, 32%, and 26.5% ($p < 0.05$) compared to that in the control. Analyzing the differences in stiffness between cells subjected to the hypoxia model and those treated with HSP70 in the nuclear region revealed two types of responses: in some points, stiffness decreased, while in others, it increased. Specifically, at points 8 and 19, the surface stiffness in cultures treated with HSP70 at a concentration of 10^{-6} M decreased by 11% and 17% ($p < 0.05$), respectively, whereas at points 14 and 17, stiffness increased by 24.5% and 19.5% ($p < 0.05$) compared to that in cells after hypoxia.

Under the influence of HSP70 at a concentration of 10^{-8} M, an increase in cell surface stiffness was established at the cell periphery in points 4, 5, and 21 compared to that in the control. In the nuclear region, a significant increase in stiffness was noted at point 17 compared to that in the control (Fig. 5).

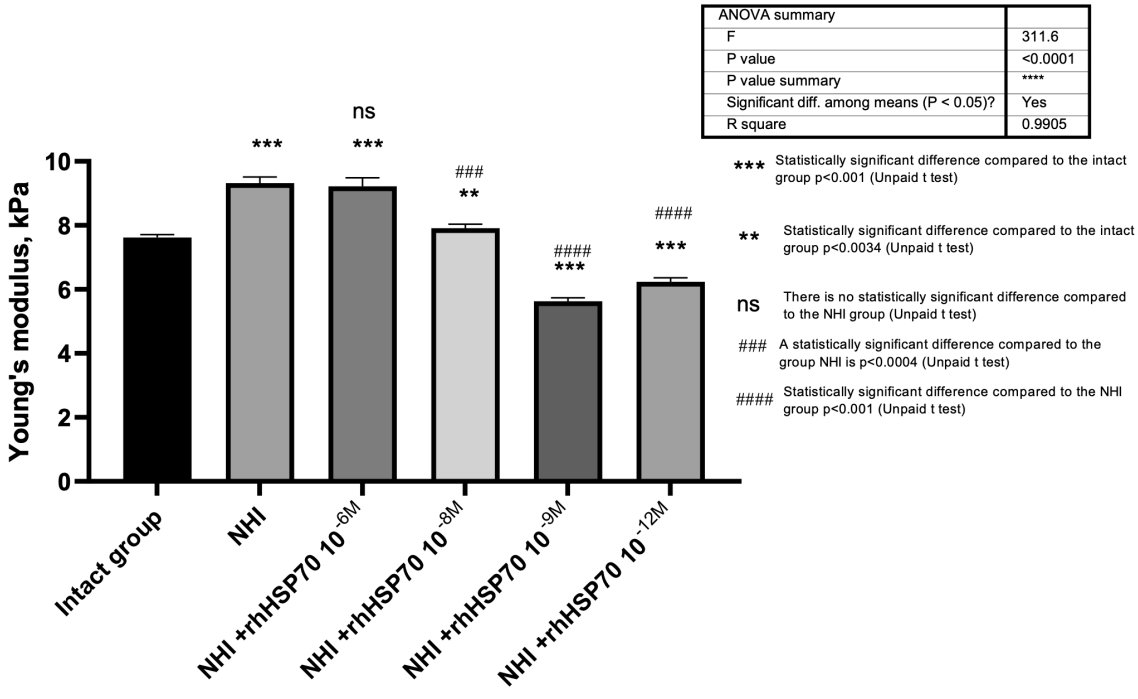

Figure 2. Young's modulus of the cell surface of primary mixed cultures of neurons in a neonatal hypoxia-ischemia model.

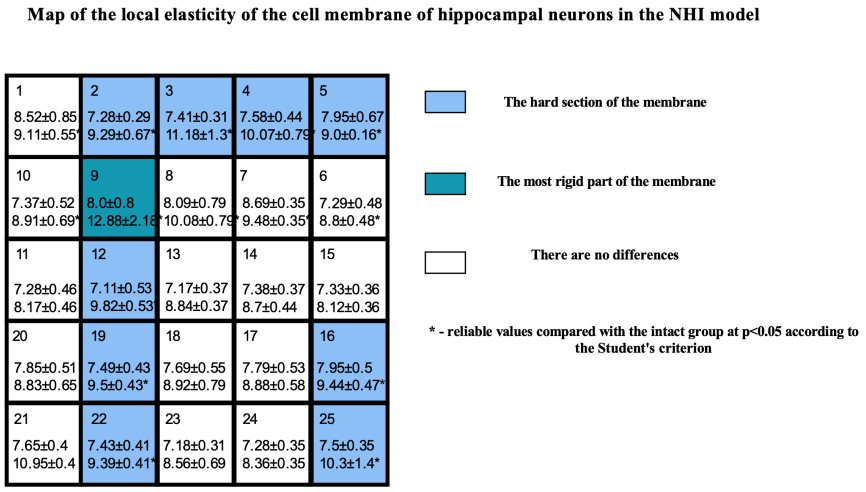

Figure 3. Local elasticity map of the neuronal cell surface in the hypoxia-ischemia model. ***Note:*** Row 1 – the control and Row 2 – data following in vivo hypoxia.

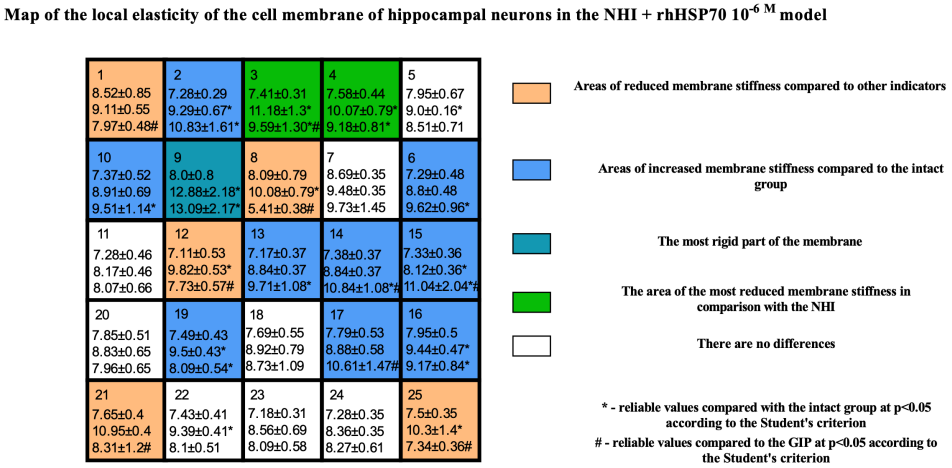

Figure 4. Local elasticity map of the neuronal cell surface in the hypoxia-ischemia model + rhHSP70 10^{-6} M. ***Note:*** Row 1 – data from the control group, Row 2 –data obtained after hypoxia, and Row 3 –data following the addition of HSP 70 at a concentration of 10^{-6} M to the neuronal cultures after hypoxia; * – indicates statistically significant values compared to those in the intact group at $p < 0.05$ according to Student's t-test. # – indicates statistically significant values compared to those in the hypoxia-ischemia group at $p < 0.05$ according to Student's t-test.

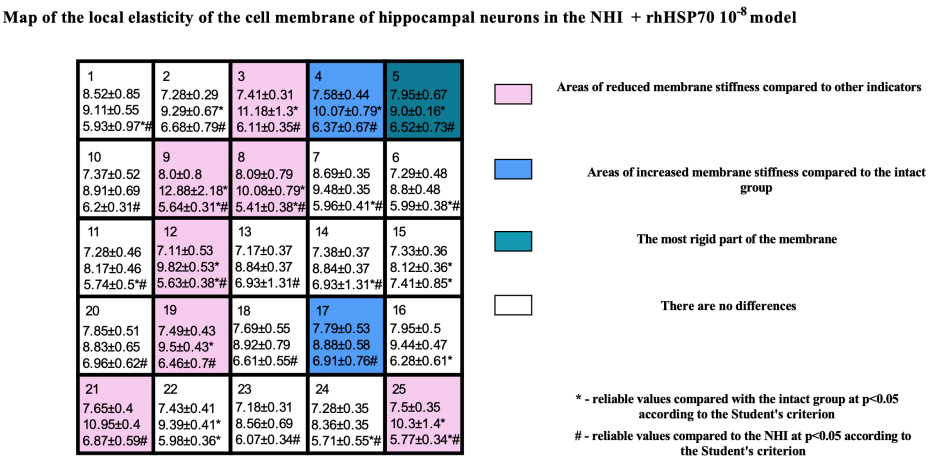

Figure 5. Local elasticity map of the neuronal cell surface in the hypoxia-ischemia model + rhHSP70 10^{-8} M. ***Note:*** Row 1 – control, Row 2 – data after hypoxia, Row 3 – data after the introduction of HSP 70 at a concentration of 10^{-8} M into neuron cultures following hypoxia; * – statistically significant values compared to the intact group at $p < 0.05$ according to the Student's t-test; # – statistically significant values compared to the HIB group at $p < 0.05$ according to the Student's t-test.

Under the influence of HSP70 at a concentration of 10^{-9} M, a decrease in the Young's modulus was observed at the cell periphery in points 1-6, 10, 11, 15, 16, and 20-25, with an average reduction of 55-63% ($p < 0.05$) compared to such in the control (Fig. 6). In the perinuclear space and nucleus, a similar decrease in cell surface stiffness was noted under the influence of HSP70. The most pronounced differences were observed at points 9 and 18.

Under the influence of HSP70 at a concentration of 10^{-12} M, a significant decrease in cell surface stiffness was observed at the periphery in points 1, 6, 11, 22, 24, and 25 compared to such in the control (Fig. 7).

The reduction in cell surface stiffness under the influence of HSP70 at the specified concentration was also observed in the perinuclear space. The most pronounced differences were noted at points 7, 8, and 9, with decreases of 46%, 49%, and 42%, respectively ($p < 0.05$) compared to such in the control.

Discussion

The relationship between the increase and decrease in membrane stiffness of neurons, investigated using atomic force microscopy (AFM), can be complex and multifaceted. Membrane stiffness is an important parameter that reflects the mechanical properties of the cell membrane and can influence numerous cellular processes, including signaling, interactions with other cells, and resistance to damage. Broadly speaking, changes in the physical properties of a neuron's membrane, in the case of increased stiffness, contribute to the stability of the cellular structure and reduce the mobility of membrane proteins. This may be beneficial for maintaining membrane integrity under mechanical stress; however, it can limit the adaptability of neurons to changes in their environment. Conversely, a decrease in

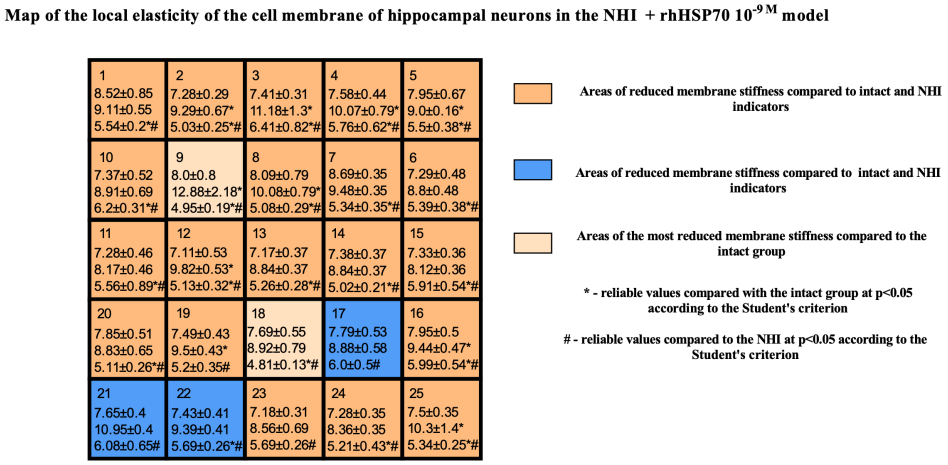

Figure 6. Local Elasticity Map of the Neuronal Cell Surface in the Hypoxia-Ischemia Model + rhHSP70 10^{-9} M. ***Note:*** Row 1 – the control group, Row 2 – data after in vivo hypoxia, Row 3 – data after the introduction of HSP 70 at a concentration of 10^{-9} M into neuron cultures following hypoxia; * – statistically significant values compared to the intact group at $p < 0.05$ according to the Student's t-test– # – statistically significant values compared to the HIB group at $p < 0.05$ according to the Student's t-test.

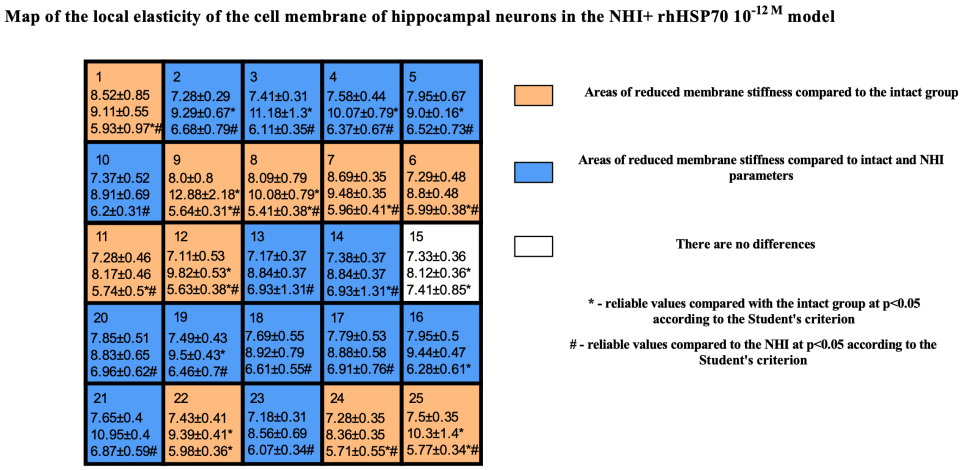

Figure 7. Local elasticity map of the neuronal cell surface in the hypoxia-ischemia model + rhHSP70 10^{-12} M. ***Note:*** Row 1 – the control group; Row 2 – the data obtained after in vivo hypoxia; Row 3 – the data following the addition of HSP 70 at a concentration of 10^{-12} M to the neuronal cultures after hypoxia; * – indicates statistically significant values compared to the intact group at $p < 0.05$ according to Student's t-test; # – indicates statistically significant values compared to the hypoxia-ischemia group at $p < 0.05$ according to Student's t-test.

stiffness allows for greater mobility of membrane proteins and flexibility of the membrane, enabling neurons to adapt more readily to changes, enhancing interactions with other cells, and promoting more efficient signaling (Kiral et al. 2018).

In the context of alterations in cellular signaling, increased membrane stiffness indicates reduced protein mobility, which may hinder signal transduction and receptor interactions, leading to impaired cellular functions and reduced neuronal plasticity. In contrast, a decrease in stiffness may facilitate more effective cellular signaling and interaction with the environment, which is crucial for the normal functioning of neurons and their capacity for adaptation (Wilson et al. 2020).

In discussing the changes in neuronal membrane properties in response to stress, an increase in membrane stiffness may represent an adaptive response to chronic stressors, such as inflammation or oxidative stress, allowing cells to maintain structural integrity. However, prolonged exposure to stress may also lead to cellular dysfunction, while a decrease in stiffness may indicate cellular dysfunction and damage, often observed in neurodegenerative diseases (Cheirdaris 2022). Nevertheless, such softness may be a temporary adaptation to acute stress conditions, enabling cells to better cope with changes.

Comparing the literature with the results of our study, it is evident that the addition of recombinant human HSP70 (rhHSP70) to primary mixed cultures of the hippocampus, obtained after modeling neonatal hypoxia-ischemia, allows neurons to adapt more easily to changes, improving interactions with other cells, which is important for the normal functioning of neurons and their adaptive capacity. This may indicate the initiation of neuronal adaptation processes to acute stress conditions, enabling cells to better handle critical situations.

Modeling neonatal hypoxia-ischemia in mice results in an 18% increase in cell surface stiffness ($p < 0.05$), which may be associated with an increase in the concentration of hypoxic shock mediators (HIF) in the damage focus, currently known as HIF-1, HIF-2, and HIF-3. These are heterodimers composed of an oxygen-sensitive α-subunit and a stable β-subunit (Tirpe et al. 2019). Under normoxic conditions, the heterodimer dissociates with the involvement of prolyl hydroxylase, which hydrolyzes two proline residues in the α-subunit of HIF-1, leading to subsequent proteasomal degradation (Dabral et al. 2019).

When HSP70 is added to the culture medium, it is established that at a concentration of 10^{-9} M, surface stiffness is maximally reduced by 65.5% ($p < 0.05$) compared to the hypoxia-ischemia group and by 35.3% ($p < 0.05$) compared to the intact group. The addition of HSP70 at a concentration of 10^{-6} M increases surface stiffness and does not differ from the model of acute hypoxia.

It is known that HSP70 regulates compensatory pathways of ATP synthesis, independently maintaining the expression of mitochondrial NAD-dependent malate dehydrogenase activity, thereby sustaining the activity of the malate-aspartate shuttle mechanism over an extended period (Belenichev et al. 2023).

Analyzing the maps of local elasticity reveals that HSP70 has a bidirectional effect on the elastic properties of the surface. It can be hypothesized that during the modeling of acute hypoxia, endogenous HSP70 appears in the extracellular space. Notably, point 9 represents a localized area of maximum stiffness located in the perinuclear space of the cell. It is known that in response to ischemia, a sharp increase in HSP70 levels is recorded, with the highest concentrations observed in vital parts of cells: the nucleus, perinuclear space, mitochondria, and endoplasmic reticulum, underscoring the importance of chaperone 70 in protection against cell death (Shao et al. 2019). As the activity of nuclear preribosomes resumes, the concentration of HSP70 in the nucleus decreases while increasing in the cytoplasm of cells. Thus, the level of HSP70 can be considered a marker of cellular and tissue damage. The hyperproduction of HSP70 in cells inhibits the development of autophagy as an alternative, more "radical" mechanism of cellular response to stress (Leu et al. 2017; Dukay et al. 2019).

The changes in cell surface stiffness we observed in various points of nanoindentation under conditions of acute hypoxia and the influence of different concentrations of HSP70 may result from alterations in the restructuring of neuronal cytoskeletal elements. There is increasing evidence that dying or damaged cells following ischemia exhibit both nuclear and cytoplasmic changes. Researchers believe that the degradation of cytoskeletal proteins is a decisive factor in the study of neuronal damage following ischemia. Interestingly, differences in processes associated with cell death, such as DNA degradation and cytoskeletal disruption, are likely to reflect varying degrees of ischemic damage; for example, mild ischemia, such as a 5-minute bilateral occlusion of the carotid arteries, caused DNA cleavage with subsequent loss of MAP-2 immunoreactivity, while ischemia, such as a 30-minute unilateral occlusion of the middle cerebral artery or complete ischemia with decapitation, led to the loss of MAP-2 immunoreactivity more rapidly than nuclear changes in the hippocampus (Nakano et al. 2019). According to the literature, in some ischemic models, MAP-2 has been proposed as a marker of cytoskeletal degradation. It has been demonstrated that cerebral ischemia can lead to the depolymerization of microtubules (Papa et al. 2018). The microtubule network is crucial for cargo transport to neuronal synapses (Mishra et al. 2024). A study (Bryniarska-Kubai et al. 2023) identified a high susceptibility of the cytoskeleton to hypoxia, including the rearrangement of actin into "sponge-like structures." Similar results were observed in an in vivo stroke model, reflected in actin depolymerization and subsequent aggregation (Guo et al. 2019). The development of neurodegenerative diseases is based on the progressive dysfunction of neurons that are unable to function individually and interact with neighboring cells, ultimately leading to various clinical phenotypes, each characteristic of a specific type of neurodegenerative disease (Levenson et al. 2014). The most common form of neurodegeneration is ischemia and hypoxic stress, which are accompanied by a range of pathological processes affecting various brain structures. Post-ischemic genetic and proteomic changes lead to neuronal death, the formation of amyloid and tau protein aggregates, progressive inflammation, and the development of brain atrophy, which may be accompanied by the onset of full-blown dementia resembling Alzheimer's disease (Pluta et al. 2021). Studies indicate that neurodegeneration characteristic of Alzheimer's disease may develop in the brain following ischemia (Pluta et al. 2019, 2021; Radenovic et al. 2020).

Neuronal death is typically preceded by subtle functional and structural changes, including synaptic damage, neurite retraction, and disruption of axonal signal transmission due to the restructuring and instability of microtubules. Instability occurs concurrently with minor molecular-level changes, such as DNA oxidation, extensive oxidation of membrane lipids, and improper protein aggregation (Qin et al. 2022). In this context, investigating the morphofunctional properties and various molecular aspects of neurodegenerative changes at the nanoscale, starting from the cell surface, is highly relevant. To address this task, contemporary biomedical research employs atomic force microscopes, which allow for the study of the topography of the cell surface with sub-nanometer resolution. Pronounced pathological conditions are accompanied by changes in the shape and adhesive properties of the cell surface. Quantitative characterization of molecular changes in biological samples related to the progression of neurodegenerative diseases provides new insights into the fundamental mechanisms underlying the onset and progression of these pathologies (Kiio and Park 2020).

Conclusion

Thus, the addition of rhHSP70 results in a decrease in membrane stiffness in mixed cultures of hippocampal neurons in comparison to both the intact group and the culture obtained after neonatal hypoxia-ischemia. The AFM method allows for the assessment of how various molecules, such as heat shock proteins (e.g., rhHSP70), influence the mechanical properties of membranes, which may be critically important for the development of new therapeutic agents.

Conflict of interest

The authors declare the absence of a conflict of interests.

Funding

This work was supported by the Ministry of Science and Higher Education of the Russian Federation, agreement No. 075-15-2021-1346, and agreement No. FZWG-2021-0016. The work was conducted with the support of the Ministry of Science and Higher Education of the Russian Federation (project No. 075-15-2021-1360).

Acknowledgments

The author expresses gratitude to M.Yu. Skorkina and A.S. Zelentsova for their consultation in planning and conducting the research.

Data availability

All of the data that support the findings of this study are available in the main text.

References

- Belenichev IF, Aliyeva OG, Popazova OO, Bukhtiyarova NV (2023) Involvement of heat shock proteins HSP70 in the mechanisms of endogenous neuroprotection: the prospect of using HSP70 modulators. Frontiers in Cellular Neuroscience 17(1): 113–168. https://doi.org/10.3389/fncel.2023.1131683 [PubMed] [PMC]
- Bryniarska-Kubiak N, Kubiak A, Trojan E, Wesołowska J, Lekka M, Basta-Kaim A (2023) Oxygen-glucose deprivation in organotypic hippocampal cultures leads to cytoskeleton rearrangement and immune activation: link to the potential pathomechanism of ischemic stroke. Cells 12: 1465. https://doi:10.3390/cells12111465 [PubMed] [PMC]
- Cartagena-Rivera AX, Wang WH, Geahlen RL, Raman A (2015) Fast, multi-frequency, and quantitative nanomechanical mapping of live cells using the atomic force microscope. Scientific Reports 5: 11692. https://doi.org/10.1038/srep11692 [PubMed] [PMC]
- Cheirdaris D (2022) Visualizing Neurodegeneration Using Atomic Force Microscopy. Handbook of Computational Neurodegeneration (4): 1–21. https://doi.org/10.1007/978-3-319-75479-6_4-2
- Chighizola M, Dini T, Lenardi C, Milani P, Podestà A, Schulte C (2019) Mechanotransduction in neuronal cell development and functioning. Biophysical reviews 11: 701–720. https://doi.org/10.1007/s12551-019-00587-2 [PubMed] [PMC]
- Dabral S, Muecke C, Valasarajan C, Schmoranzer M, Wietelmann A, Semenza GL, Meister M, Muley T, Seeger-Nukpezah T, Samakovlis C, Weissmann N, Grimminger F, Seeger W, Savai R, Pullamsetti SS (2019) A RASSF1A-HIF1α loop drives Warburg effect in cancer and pulmonary hypertension. Nature Communications 10(1): 2130 https://doi.org/10.1038/s41467-019-10044-z [PubMed] [PMC]
- DeGiosio RA, Grubisha MJ, MacDonald ML, McKinney BC, Camacho CJ, Sweet RA (2022) More than a marker: Potential pathogenic functions of MAP2. Frontiers in Molecular Neuroscience 15: 974890. https://doi.org/10.3389/fnmol.2022.974890 [PubMed] [PMC]
- Demyanenko S, Nikul V, Rodkin S, DavletsHIn A, Evgen'ev MB, Garbuz DG (2021) Exogenous recombinant Hsp70 mediates neuroprotection after photothrombotic stroke. Cell Stress and Chaperones 26(1): 103–114. https://doi.org/10.1007/s12192-020-01159-0 [PubMed] [PMC]
- Dukay B, Csoboz B, Tóth ME (2019) Heat-shock proteins in neuroinflammation. Frontiers in Pharmacology 10: 920–931 https://doi.org/10.3389/fphar.2019.00920 [PubMed] [PMC]
- Frederix PL, Bosshart PD, Engel A (2009) Atomic force microscopy of biological membranes. Biophysical Journal 96(2): 329–338. http://doi.org/10.1016/j.bpj.2008.09.046 [PubMed] [PMC]
- Galvanetto N (2018) Single-cell unroofing: probing topology and nanomechanics of native membranes. Biochim Biophys Acta (BBA) – Biomembranes 1860: 2532–2538. https://doi.org/10.1016/j.bbamem.2018.06.011 [PubMed]
- Guimarães CF, Gasperini L, Marques AP, Reis RL (2020) The stiffness of living tissues and its implications for tissue engineering. Nature Reviews Materials 5: 351–370. https://doi.org/10.1038/s41578-019-0120-8
- Guo CY, Xiong TQ, Tan BH, Gui Y, Ye N, Li SL, Li YC (2019) The temporal and spatial changes of actin cytoskeleton in the hippocampal CA1 neurons following transient global ischemia. Brain research 17(20): 1462–1497. https://doi:10.1016/j.brainres.2019.06.016 [PubMed]
- Guo CY, Xiong TQ, Tan BH, Gui Y, Ye N, Li SL, Li YC (2019) The temporal and spatial changes of actin cytoskeleton in the hippocampal CA1 neurons following transient global ischemia. Brain Research 1720: 146297. https://doi.org/10.1016/j.brainres.2019.06.016 [PubMed]
- Handorf AM, Zhou Y, Halanski MA, Li W-J (2015) Tissue stiffness dictates development, homeostasis, and disease progression. Organogenesis 11(1): 1–15. https://doi.org/10.1080/15476278.2015.1040571 [PubMed] [PMC]
- Kiio TM, Park S (2020) Nano-scientific application of atomic force microscopy in pathology: from molecules to tissues. International journal of medical sciences17: 844–858. https://doi.org/10.7150/ijms.41805 [PubMed] [PMC]
- Kiral FR, Kohrs FE, Jin EJ, Hiesinger PR (2018) Rab GTPases and membrane trafficking in neurodegeneration. Current Biology 28(8): 471–486. https://doi.org/10.1016/j.cub.2018.02.010 [PubMed] [PMC]
- Leu JI, Barnoud T, Zhang G, Tian T, Wei Z, Herlyn M (2017) Inhibition of stress-inducible HSP70 impairs mitochondrial

proteostasis and function. Oncotarget 8(28): 45656–45669. https://doi.org/10.18632/oncotarget.17156 [PubMed] [PMC]
- Levenson RW, Sturm VE, Haase CM (2014) Emotional and behavioral symptoms in neurodegenerative disease: a model for studying the neural bases of psychopathology. Annual review of clinical psychology 10: 581–606. https://doi.org/10.1146/annurev-clinpsy-032813-153653 [PubMed] [PMC]
- Mishra AK, Tripathi MK, Kumar D, Gupta SP (2024) Neurons specialize in presynaptic autophagy: A perspective to ameliorate neurodegeneration. Molecular Neurobiology https://doi.org/10.1007/s12035-024-04399-8 [PubMed]
- Nakano F, Liu L, Kawakita F, Kanamaru H, Nakatsuka Y, Nishikawa H, Okada T, Shiba M, Suzuki H (2019) Morphological characteristics of neuronal death after experimental subarachnoid hemorrhage in mice using double immunoenzymatic technique. The Journal of Histochemistry and Cytochemistry 67(12): 919–930. https://doi.org/10.1369/0022155419878181 [PubMed] [PMC]
- Ohashi K, Fujiwara S, Mizuno K (2017) Roles of the cytoskeleton, cell adhesion and Rho signaling in mechanosensing and mechanotransduction. The Journal of Biochemistry 161(3): 245–254 https://doi.org/10.1038/s41578-019-0169-1 [PubMed]
- Papa L, Robicsek SA, Brophy GM, Wang KK, Hannay HJ, Heaton S, Schmalfuss I, Gabrielli A, Hayes RL, Robertson CS (2018) Temporal profile of microtubule-associated protein 2: A novel indicator of diffuse brain injury severity and early mortality after brain trauma. Journal of Neurotrauma 35(1):32–40. https://doi.org/10.1089/neu.2017.4994 [PubMed] [PMC]
- Pluta R, Ouyang L, Januszewski S, Li Y, Czuczwar SJ (2021) Participation of amyloid and tau protein in post-ischemic neurodegeneration of the hippocampus of a nature identical to Alzheimer's disease. International Journal of Molecular Sciences 22: 2460. https://doi.org/10.3390/ijms22052460 [PubMed] [PMC]
- Pluta R, Ułamek-Kozioł M, Januszewski S, Czuczwar SJ (2019) Amyloid pathology in the brain after ischemia. Folia Neuropathologica 57(3): 220–226. https://doi.org/10.5114/fn.2019.88450 [PubMed]
- Qin C, Yang S, Chu YH, Zhang H, Pang XW, Chen L, Zhou LQ, Chen M, Tian DS, Wang W (2022) Signaling pathways involved in ischemic stroke: molecular mechanisms and therapeutic interventions. Signal Transduction and Targeted Therapy 7: 215. https://doi.org/10.1038/s41392-022-01064-1 [PubMed] [PMC]
- Radenovic L, Nenadic M, Ułamek-Kozioł M, Januszewski S, Czuczwar SJ, Andjus PR, Pluta R (2020) Heterogeneity in brain distribution of activated microglia and astrocytes in a rat ischemic model of Alzheimer's disease after 2 years of survival. Aging 12(12): 12251–12267. https://doi.org/10.18632/aging.103411 [PubMed] [PMC]
- Seano G, Nia HT, Emblem KE, Datta M, Ren J, Krishnan S, Kloepper J, Pinho MC, Ho WW, Ghosh M (2019) Solid stress in brain tumours causes neuronal loss and neurological dysfunction and can be reversed by lithium. Nature Biomedical Engineering 3: 230–245. https://doi.org/10.1038/s41551-018-0334-7 [PubMed] [PMC]
- Shao A, Zhou Y, Yao Y, Zhang W, Zhang J, Deng Y (2019) The role and therapeutic potential of heat shock proteins in haemorrhagic stroke. Journal of Cellular and Molecular Medicine 23(9): 5846–5858. https://doi.org/10.1111/jcmm.14479 [PubMed] [PMC]
- Sheldon RA, Windsor C, Ferriero DM (2018) Strain-related differences in mouse neonatal hypoxia-ischemia. International Journal of Developmental Neuroscience 40(5-6): 490–496. https://doi.org/10.1159/000495880 [PubMed] [PMC]
- Skorkina MYu, Fedorova MZ, Sladkova EA, Muravyov AV (2012) The use of nanomechanic sensor for studies of morphofunctional properties of lymphocytes from healthy donors and patients with chronic lymphoblastic leukemia. Bulletin of Experimental Biology and Medicine 154(1): 163–166. https://doi.org/10.1007/s10517-012-1899-x [PubMed]
- Sun YY, Zhu HJ, Zhao RY, Zhou SY, Wang MQ, Yang Y, Guo ZN (2023) Remote ischemic conditioning attenuates oxidative stress and inflammation via the Nrf2/HO-1 pathway in MCAO mice. Redox Biology 66: 102852. https://doi.org/10.1016/j.redox.2023.102852 [PubMed] [PMC]
- Tirpe AA, Gulei D, Ciortea SM, Crivii C, Berindan-Neagoe I (2019) Hypoxia: overview on hypoxia-mediated mechanisms with a focus on the role of HIF genes. International Journal of Molecular Sciences 20(24): 6140. https://doi.org/10.3390/ijms20246140 [PubMed] [PMC]
- Tuo Q, Zhang S, Lei P (2021) Mechanisms of neuronal cell death in ischemic stroke and their therapeutic implications. Medicinal Research Reviews 42:259–305. https://doi.org/10.1002/med.21773 [PubMed]
- Vining KH, Mooney DJ (2017) Mechanical forces direct stem cell behavior in development and regeneration. Nature Reviews Materials 18(12): 728–742. https://doi.org/10.1038/nrm.2017.81 [PubMed] [PMC]
- Wilson KA, MacDermott-Opeskin HI, Riley E, Lin Y, O'Mara ML (2020) Understanding the link between lipid diversity and the biophysical properties of the neuronal plasma membrane. Biochemistry 59(33): 3010–301. https://doi.org/10.1021/acs.biochem.0c00524 [PubMed]
- Wilson KA, MacDermott-Opeskin HI, Riley E, Lin Y, O'Mara ML (2020) Understanding the link between lipid diversity and the biophysical properties of the neuronal plasma membrane. Biochemistry. 59(33): 3010–3018 https://doi.org/10.1021/acs.biochem.0c00524 [PubMed]

Author contributions

- **Vladimir M. Pokrovsky**, Junior Researcher at the Institute of Pharmacology of Living Systems; e-mail: vmpokrovsky@yandex.ru; **ORCID ID:** https://orcid.org/0000-0003-3138-2075. The author participated in the conceptualization and development of the research direction, defining key goals and objectives, conducting experimental work, analyzing materials, and writing the article.

- **Alexey V. Deikin**, PhD in Medical Sciences, Associate Professor of the Department of Pharmacology and Clinical Pharmacology at Belgorod State National Research University, Belgorod, Russia; e-mail: deykin@bsu.edu.ru; **ORCID ID:** https://orcid.org/0000-0001-9960-0863. The author participated in the development of the research direction and material analysis.

- **T. Zhang**, College of Life Sciences, Dezhou University, Dezhou, 253023, China; **ORCID ID:** https://orcid.org/0009-0002-5289-7617. The author participated in the development of the research direction and material analysis.

- **Nikolai A. Verlov**, PhD in Biological Sciences, Head of the Resource Center of the Molecular and Radiation Biophysics Department; **ORCID ID:** https://orcid.org/0000-0002-3756-0701. The author participated in the development of the research direction and material analysis.

- **Andrey L. Konevega**, Head of Division (Molecular and Radiation Biophysics Division); e-mail: konevega_al@spbstu.ru; **ORCID ID:** https://orcid.org/0000-0003-0125-7150. The author contributed to the collection, analysis, and interpretation of data for the article.

- **Mikhail V. Korokin**, Doctor of Medical Sciences, Professor of the Department of Pharmacology and Clinical Pharmacology at Belgorod State National Research University, Belgorod, Russia; e-mail: mkorokin@mail.ru; **ORCID ID:** https://orcid.org/0000-0001-5402-0697. The author participated in the development of the research direction and material analysis.